

# Coherent superposition of emitted and resonantly scattered photons from a two-level system driven by an even- $\pi$ pulse

I.V. Krainov,<sup>1,\*</sup> A.I. Galimov,<sup>1</sup> M.V. Rakhlin,<sup>1</sup> A.A. Toropov,<sup>1</sup> and T.V. Shubina<sup>1</sup>

<sup>1</sup>*Ioffe Institute, 194021 St. Petersburg, Russia*

(Dated: July 9, 2025)

We report the observation of a bunching of  $\sim 3$  photon states, which is a coherent superposition of emitted photons and resonantly scattered laser photons, arising upon excitation by even- $\pi$  pulses of a two-level system represented by a charged quantum dot in a microcavity. This phenomenon emerges because the exciting laser pulse contains several tens of photons whose quantum amplitude distribution creates such a superposition, and the polarization of the scattered photons is changed by the interaction with the charged resonant system. Such a beam is a high-order member of the Fock space, promising for quantum technologies.

A typical two-level system – a semiconductor quantum dot (QD) embedded in a microcavity is a promising resource for quantum technologies, capable of producing both single-photon Fock states [1–3] and multiphoton entangled states [4, 5], i.e., higher-order terms of the Fock space, which have significantly advanced quantum mechanics [6]. It is worth noting that efficient optical quantum computing can be realized using both single-photon [7] and coherent states [8], despite their semiclassical nature. N00N states, a superposition of entangled states reminiscent of Schrödinger’s cat [9], can be obtained by interference of quantum light with a coherent state [10]. Decoy states, which are intentionally added multiphoton states, including coherent ones, to a sequence of single photons, are an important tool for secure quantum key distribution [11]. Thus, the sharp boundary in applications of quantum light and classical coherent light is illusory, and different superpositions may be of interest.

The optical response of the QD-microcavity system strongly depends on the excitation type, regardless of whether the process is resonant fluorescence or resonant Rayleigh scattering [12–14]. A well-established method that ensures high purity and indistinguishability of single photons is resonant excitation with a  $\pi$ -pulse followed by cross-polarization filtering of the exciting laser light [15–17]. Even in this case, unwanted multiphoton generation may occur [18, 19], reflecting the diversity of states in the Fock space [20]. From a physical point of view, the change in photon statistics can be caused by a nonlinear process [13], mean field fluctuation and cavity dissipation [21–23], and also by the emission of a pair of photons for a single laser pulse [19, 24].

The most convincing experiments on paired photon generation were performed with  $2\pi$ -pulse excitation. Fischer et al. [19] showed that emission from a charged InAs/GaAs QD exhibits antibunching with a second-order correlation function  $g^{(2)}(0) \approx 0$  when excited by a  $\pi$ -pulse and bunching with  $g^{(2)}(0) \sim 2$  when excited by a  $2\pi$ -pulse. An intuitive theoretical explanation, supported by the quantum trajectory method [25], suggests

that two-photon emission events, stimulated by reemission, can occur during decay of excited trion state. It was also noted that the emission of photon pairs is hampered for short  $2\pi$  pulses ( $\sim 20$  ps). Subsequently, Loredó et al. [24], by embedding such a charged QD in a microcavity, enhanced the multiphoton generation. They showed that the output wave packet can be a quantum superposition of vacuum, one and two photons in a proportion depending on the pulse area. It was also noted that this superposition can be considered as a Schrödinger cat state.

In all the above-mentioned seminal works, the laser pulse is treated as a classical field, while in fact it consists of many coherent photons. Furthermore, as noted but not explained, significant multiphoton generation upon excitation by an even- $\pi$  pulse occurs only when the QD hosts a charged exciton, not a neutral exciton [24]. This stimulates further studies to clarify the mechanism of multiphoton generation in the QD-microcavity system.

In this Letter we report a study of even- $\pi$  pulsed multiphoton generation in a charged QD in a microcavity, which appears to reproduce previous data ( $g^{(2)}(0) \approx 3$ ), but clearly demonstrates that the bunching includes scattered laser photons not observed before. The cornerstone of the proposed model is the definition of a laser pulse as a wave packet consisting of several tens of photons, the distribution of the quantum amplitude of which allows them to either contribute to the excitation of a trion in a QD or resonantly scatter with the loss of the initial polarization. This leads to the creation of a quantum superposition of photons of different nature.

We have performed an experimental study using an InAs/GaAs QD in a micropillar cavity as a two-level system. The QD contains a resident hole, so the created exciton is positively charged (positive trion). The cross-polarization measurement scheme shown in Fig. 1a provides attenuation of the exciting laser light by six orders of magnitude [17]. For resonant excitation, the pulse duration of 16 ps was chosen, which contains about 50 coherent photons. Details of sample fabrication and measurements are given in Appendix A.

For the  $\pi$ -pulse excitation, we observe photon antibunching with  $g^{(2)}(0) = 0.05 \pm 0.01$  (Fig. 1b), confirming the dominance of single-photon emission. For the  $2\pi$ -

\* igor.krainov@mail.ru

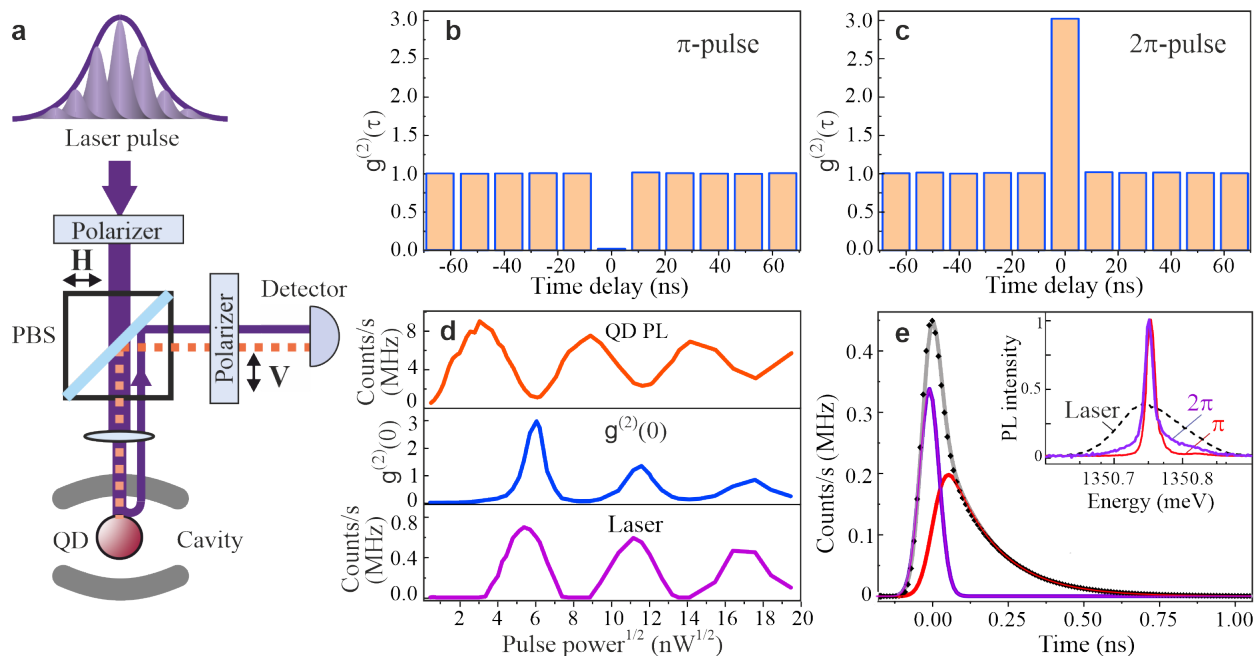


FIG. 1. (a) Experiment: The InAs/GaAs QD in the microcavity is resonantly excited by a H-polarized 16-ps laser pulse containing about 50 photons. A cross-polarization scheme with a polarizing beam splitter (PBS) allows only V-polarized light to pass to a single-photon detector. (b,c) Second-order correlation function  $g^{(2)}(\tau)$  of QD emission excited by  $\pi$ -pulse (b) and  $2\pi$ -pulse (c). (d) Oscillatory dependencies of the PL intensity,  $g^{(2)}(0)$  and the scattered laser radiation intensity as functions of excitation pulse power. (e) Time-resolved PL decay curve for  $2\pi$  excitation and its decomposition into fast laser component and slow trion emission with a characteristic decay time of 155 ps. The inset shows narrow lines of  $\pi$ -pulse excited PL and  $2\pi$ -pulse excited PL with scattered light wings. Laser pulse shape is shown for comparison.

pulse, we register a bunching with  $g^{(2)}(0) \approx 3.0 \pm 0.3$  (Fig. 1c), close to that previously published in [24], although the excitation pulses used are too short to create a photon pair [19].

Figure 1d shows the photoluminescence (PL) intensity versus pulse power, which has maxima at odd  $\pi$ -pulses and minima at even  $\pi$ -pulses, as expected for a photon emission probability controlled by the pulse area. While  $g^{(2)}(0)$  shows extremes at the opposite  $\pi$ -multiplicity. This Fig. 1d shows also a noticeable admixture of laser photons at even  $\pi$ -multiplicity, despite the very strong suppression of H-polarized laser light, almost to zero. This dependence is obtained by modeling time-resolved PL decay curves as described in Appendix A. The PL kinetics are characterized by a rapidly decaying laser component, absent at odd  $\pi$ -multiplicity, and a slower trion emission component (Fig. 1e). Under the experimental conditions used, the admixture of laser photons can be explained only by their resonant scattering with the loss of the original polarization. The emission lines excited by the  $\pi$  and  $2\pi$  pulses have practically the same width  $\sim 10 \mu\text{eV}$  (Fig. 1e, inset), noticeably narrower than the laser pulse, which is a sign of a tight resonant interaction with the two-level system. In addition, the  $2\pi$  line has wings of scattered light. Their integral intensity is close to the intensity of the narrow component, which indicates an almost equal probability of two resonant processes -

trion emission and photon scattering.

To clarify the influence of the microcavity on these two processes, we conducted an experiment on the detuning of the QD radiation energy and the cavity mode energy. Such a detuning was achieved by various shifts in these energies with increasing temperature. With detuning, we observe a decrease in the Purcell factor, which is manifested in an increase in the characteristic trion PL decay time from 155 ps to 800 ps (Fig. 2a). Accordingly, the photon statistics changes from super-Poissonian to Poissonian (Fig. 2b).

To create a model that explains our results, we first consider the ideal QD-microcavity system without dephasing. The cavity mode is assumed to be a doubly degenerate fundamental mode with energy  $\hbar\omega_0$  matching the trion transition energy  $E_t$ . The system is resonantly excited, i.e. the laser energy  $\hbar\omega_L$  corresponds to  $E_t$ . For definiteness, we assume that the hole has a spin state  $|+3/2\rangle$  (the opposite sign will not change the form of the derived expressions). During the long hole lifetime  $\geq 5$  ns in InAs/GaAs QDs [26] only the optical transition  $\sigma_-$  is active, controlled by the Hamiltonian

$$\hat{H}_0 = g \left( \hat{b}_-^\dagger \hat{a}_+ + \hat{b}_- \hat{a}_+^\dagger \right), \quad (1)$$

where  $\hat{b}_i^\dagger$  is the photon cavity mode creation operator with polarization  $i = \text{H}, \text{V}, \pm$ ;  $\hat{b}_\pm^\dagger = (\hat{b}_H^\dagger \pm i\hat{b}_V^\dagger)/\sqrt{2}$ ;  $\hat{a}_+$

is the creation operator for a positively charged trion with a spin-up electron;  $g$  is the coupling constant. Here, the rotating-wave approximation is applied. The key aspect of the generation of a multiphoton state at such conditions is the multiphoton nature of the pump pulse. In a linear cross-polarized configuration (H-polarized pump, V-polarized detection), the H-polarized pump pulse is a coherent superposition of photons:

$$|\Psi_{\text{in}}\rangle = e^{-|\alpha|^2/2} e^{\alpha \hat{b}_H^\dagger} |0\rangle = e^{-|\alpha|^2/2} \sum_n \frac{\alpha^n}{\sqrt{n!}} |n_H\rangle, \quad (2)$$

where  $|\alpha|^2 = N$  is the mean photon number in the pulse. Under resonant excitation, the interaction between the pump pulse and the trion is described by the evolution operator  $\hat{S}_0 = \exp(-i\tau\hat{H}_0)$ , where  $\tau$  is the interaction time between the trion and the pulse. This time is defined by the duration of the pulse  $\tau_p$  and the width of the cavity mode  $\Gamma$  as  $\tau = \max(\tau_p, \hbar/\Gamma)$ . It depends also on detuning between pumping laser and cavity mode as discussed later.

Monochromatic linearly polarized (H) light can be represented as a combination of two circularly polarized components  $e_H = (\sigma_+ + \sigma_-)/\sqrt{2}$ . The interaction of the considered trion state and the light component  $\sigma_-$  leads to Rabi oscillations with frequency  $\Omega_R \sim g\sqrt{n}$ . The distribution of the number of photons in the input pulse leads to a superposition of coherent states oscillating at different frequencies. This leads to a non-zero probability of excitation of the trion state for a  $2\pi$ -pulse. The outgoing state is

$$\begin{aligned} |\Psi_{\text{out}}\rangle &= \hat{S}_0 |\Psi_{\text{in}}\rangle = e^{-|\alpha|^2/2} e^{\alpha \hat{b}_+^\dagger/\sqrt{2}} \hat{S}_0 e^{\alpha \hat{b}_-^\dagger/\sqrt{2}} |0\rangle \approx \\ &\approx \frac{e^{-|\alpha|^2/2} e^{\alpha \hat{b}_H^\dagger}}{2} \left[ \left( e^{i\theta/2} e^{i\delta \hat{b}_-^\dagger} + e^{-i\theta/2} e^{-i\delta \hat{b}_-^\dagger} \right) - \right. \\ &\quad \left. - \left( e^{i\theta/2} e^{i\delta \hat{b}_-^\dagger} - e^{-i\theta/2} e^{-i\delta \hat{b}_-^\dagger} \right) \hat{a}_+^\dagger \right] |0\rangle, \quad (3) \end{aligned}$$

where  $\theta = g\tau\sqrt{N}$  represents the pulse area,  $\delta = g\tau\alpha/2\sqrt{2N}$ . In this equation, we linearize  $\sqrt{n}$  around  $N$  for large mean photon numbers ( $N \gg 1$ ). It is seen that the wave function of the system has additions to the vacuum and trion states (area theorem). Such additions are symmetric and antisymmetric Schrödinger cat states with phase  $\delta$ .

After the pulse excitation, the trion emits a  $\sigma_-$  photon, so we replace the trion creation operator with a photon  $\hat{a}_+^\dagger \rightarrow \hat{b}_-^\dagger$ . The detection scheme uses a cross-polarized (V) projection of the output state

$$\begin{aligned} |\Psi_{\text{out}}^V\rangle &\approx \cos\left(\frac{\theta}{2}\right) |0\rangle - \frac{i+\delta}{\sqrt{2}} \sin\left(\frac{\theta}{2}\right) |1\rangle - \\ &\quad - \frac{i\delta}{2} \cos\left(\frac{\theta}{2}\right) |2\rangle, \quad (4) \end{aligned}$$

where we retain only first-order terms in  $\delta \sim g\tau \ll 1$ . The state  $|2\rangle = \hat{b}_-^\dagger \hat{b}_-^\dagger |0\rangle$  is a two-photon state, one of

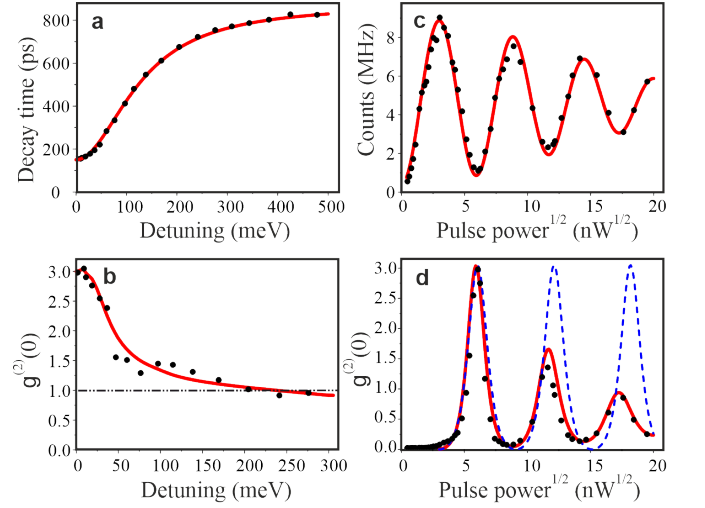


FIG. 2. Comparison of experimental (dots) for resonant excitation by  $2\pi$ -pulse and calculated dependencies ( $\theta = 2\pi$ ). Red curves — simulation using the full model, blue — without damping effects, eq. (5). (a) Trion lifetime vs detuning  $\Delta = \hbar\omega_0 - E_t$ . Simulation is performed at  $\nu_0\Gamma = 0.55$ . (b)  $g^{(2)}(0)$  vs detuning. Simulation is performed at  $\Gamma\tau_p = 1.5$ ; other parameters from (a,c,d). (c) Rabi oscillations in QD radiation as a function of pulse area. The simulation is performed with  $2\gamma\tau = 0.003\theta^2$ ,  $\theta = \theta + 0.0027\theta^2$ . (d)  $g^{(2)}(0)$  as a function of the pulse area. The simulation is performed with  $\delta = 0.58$ ,  $\lambda = 0.08$ ,  $\gamma_1 = 0.17$ ,  $\gamma_2 = 0$ . The rest parameters are the same as in (c). The fitting details are given in Appendix C.

which is a laser photon resonantly scattered by the trion, and the other is a photon arising from trion recombination. Note that these two-photon states oscillate coherently with the pulse area, participating in oscillations in the second-order correlation function. The zero-delay second-order correlation function for the output state (4) reads as

$$g^{(2)}(0) = \frac{\langle \Psi_{\text{out}}^V | \hat{n}^2 - \hat{n} | \Psi_{\text{out}}^V \rangle}{\langle \Psi_{\text{out}}^V | \hat{n} | \Psi_{\text{out}}^V \rangle^2} = \frac{2|\delta|^2 \cos^2\left(\frac{\theta}{2}\right)}{(\sin^2\left(\frac{\theta}{2}\right) + |\delta|^2)^2}. \quad (5)$$

Equation (5) exhibits the oscillatory dependence of  $g^{(2)}(0)$  on the pump pulse area. Notably,  $g^{(2)}(0)$  vanishes for odd pulse areas ( $\pi, 3\pi, \dots$ ) and peaks at  $2/\delta^2$  for even areas ( $2\pi, 4\pi, \dots$ ). This behavior demonstrates that the multiphoton states originate from fully coherent dynamics. This equation assumes  $N \gg 1$  and is not valid for the pulse area near zero, where this effect is absent. For a fixed pump energy, the correlation function exhibits damped oscillations with increasing pulse duration  $\tau$ . As the pump power increases, at a fixed  $\tau$ , it should exhibit undamped oscillations.

The experimentally observed decrease in  $g^{(2)}(0)$  with increasing pump power at a fixed  $\tau$  indicates the influence of phonons [27, 28]. To model this, we derive density matrix equations assuming weak coupling with acoustic phonons. The full Hamiltonian consists

of three components:  $\hat{H}_0$  describes the electron-photon system considered above,  $\hat{H}_p = \sum_k \omega_k \hat{c}_k^\dagger \hat{c}_k$  represents free phonons, and  $\hat{H}_i = \hat{a}_+^\dagger \hat{a}_+ \sum_k t_k (\hat{c}_k^\dagger + \hat{c}_k)$  takes into account the trion-phonon interaction with the coupling constant  $t_k$ ,  $\hat{c}_k^\dagger$  creates phonons in the mode  $k$  with dispersion  $\omega_k = ck$ .

Following the established procedure [28], we consider phonon-induced dephasing using a second-order perturbation theory. In Appendix B, we present the solution of the master Lindblad equation, where phonons determine two parameters: the phonon-induced decay rate  $\gamma$  and a small correction  $\varepsilon$  to the Rabi frequency [29]. We consider a high-temperature regime ( $T \gg \Omega_R$ ), in which  $\gamma \sim \Omega_R^2$  leads to the decay of both Rabi oscillations and  $g^{(2)}(0)$ . The solution for the trion dynamics after a laser pulse with interaction with the phonon bath  $\hat{\rho}_\tau$  is given by Eq. (B8) in Appendix B. To account for experimental imperfections, we introduce an incoherent admixture  $\lambda$  into the output state, yielding a total density matrix  $\hat{\rho}_{\text{tot}} = (1 - \lambda)\hat{\rho}_\tau + \lambda\hat{\rho}_{\text{mix}}$ , where  $\lambda$  participates in two parameters:  $\gamma_1 = 2\lambda \text{Tr}[\hat{\rho}_{\text{mix}}\hat{n}]/(1 - \lambda)$ ,  $\gamma_2 = 4\lambda \text{Tr}[\hat{\rho}_{\text{mix}}(\hat{n}^2 - \hat{n})]/(1 - \lambda)$ . Applying the same procedure as before, we derive the second-order correlation function:

$$g^{(2)}(0) = \frac{4|\delta|^2 \left(1 + e^{-2\gamma\tau} \cos(\tilde{\theta})\right) + \gamma_2}{\left(1 - e^{-2\gamma\tau} \cos(\tilde{\theta}) + 2|\delta|^2 + \gamma_1\right)^2 (1 - \lambda)}, \quad (6)$$

where  $\tilde{\theta} = \theta - \varepsilon\tau$ . The quadratic dependence  $\gamma \sim \theta^2$  explains the observed decay of  $g^{(2)}(0)$  with increasing pump power, as well as the damping of Rabi oscillations  $P_{\text{trion}} = [1 - e^{-2\gamma\tau} \cos(\tilde{\theta})]/2$ .

To verify our model, we investigate its ability to describe multiphoton states when the interaction between the trion and the cavity mode is varied. To do so, we introduce an energy detuning between the cavity mode and the trion transition defined as  $\Delta = \hbar\omega_0 - E_t$ , keeping the fixed pulse area and resonant excitation  $\hbar\omega_L = E_t$ , which corresponds to the experimental conditions for obtaining the data in Fig. 2b. For  $\theta = 2\pi$  and assuming  $\gamma\tau \sim \Omega_R^2\tau = \theta^2/\tau$ , the Eq. (6) reads as

$$g^{(2)}(0) \approx \frac{2|\delta|^2}{(|\delta|^2 + b\theta^2/\tau)^2}. \quad (7)$$

When phonon dephasing dominates, the parameter  $b \propto T$ . The interaction time  $\tau$  and the coupling strength  $\delta$  depend on the detuning through a change in the photon density of states, which is affected by the energy width of the cavity mode  $\Gamma$  and the density of states outside the mode  $\nu_0$ . They influence the Purcell factor controlling the trion decay time (Fig. 2a). For zero detuning and neglecting the residual photon density of states  $\nu_0$ , the interaction time is  $\tau = \tau_p + \hbar/\Gamma = \max(\tau_p, \hbar/\Gamma)$ , where  $\tau_p$  is the laser pulse duration. When detuned, its dependence is described by a function of  $\Delta$ ,  $\Gamma$ ,  $\nu_0$ ,  $\tau_p$ . Substituting Eqs (C2), (C3) into (6), we obtain the dependence of  $g^{(2)}(0)$  on the detuning for  $\theta = 2\pi$  (see Appendix C).

The fitting of the experimental data presented in Fig. 2 is performed using the procedure described in Appendix C. The obtained theoretical dependence of  $g^{(2)}(0)$  for  $\theta = 2\pi$  on the detuning (Fig. 2b) shows a change from super-Poissonian to Poissonian statistics, as does the experimental dependence. In short, the detuning suppresses the resonant excitation of the trion and hence shifts the balance in favor of resonantly scattered coherent photons. In addition, decreasing the Purcell gain weakens the nonlinear effects that can contribute to the photon polarization rotation [30–32]. Overall, Fig. 2 shows that we can modify the photon statistics of such multiphoton states in two ways: by detuning the energy and by changing the pulse power.

The significance of the developed model goes beyond the efficient simulation of experimental dependencies. Its key ideas can be useful for looking at previous landmark studies from a different angle. For example, the intuitive theory of multiphoton generation under even- $\pi$  excitation [19] can be formalized taking into account the multiphoton nature of the pump pulse. The cavity-enhanced polarization rotation by the trion in the QD [30, 31] is consistent with the appearance of an antisymmetric term in equation 3. Also, the predicted output signal with two probabilistic terms, the additions, resembles the Schrödinger's cat state discussed in [24].

In summary, we have demonstrated that multiphoton emission from a charged QD in a microcavity excited by an even- $\pi$  pulse is a quantum superposition of single photons emitted by the QD and resonantly scattered pump photons. The established oscillatory dependence of  $g^{(2)}(0)$  and other characteristics on the pulse area is a distinctive feature of coherent multiphoton dynamics. Our findings indicate that the measured second-order correlation function  $g^{(2)}(0) \approx 3$  does not necessarily imply the dominance of photon-pair emission, which was previously considered as the main mechanism for that.

We developed a theory describing the generation of such quantum states, which is based on two key conditions: the multiphoton nature of the pump pulse and the presence of a charged exciton (trion) in the QD. Together, they lead to a coherent superposition of emitted and scattered photons, which is a high-order member of the Fock space. Including phonon-induced dephasing and incoherent noise in this model allowed us to accurately reproduce the observed Rabi oscillations, as well as the second-order correlation function with and without energy detuning. The key ideas of this model allow one to provide a unified interpretation of the previous results.

This study provides compelling evidence that coherent pulsed light interacting with a QD-microcavity system can generate non-classical light with tunable photon statistics, which is in line with ongoing research aimed at creating scalable excitation field-controlled photonic architectures. From a practical perspective, such multiphoton states combining photons of different natures can be used in quantum computing and quantum key distribution protocols.

## Appendix A: Experimental details

The sample under study is a micropillar with a diameter of 3  $\mu\text{m}$ , made of a heterostructure with distributed Bragg reflectors grown by molecular beam epitaxy. It consists of 30 (18) lower (upper) pairs of  $\lambda/4$  GaAs/AlGaAs layers and a positively charged InAs/GaAs QD emitting at 920 nm in the  $\lambda$  cavity between them. Details of the technology can be found in [33]. During the experiments, the sample was placed in a cryostat with a minimum temperature of 9 K. Its radiation was collected and directed to a superconducting single-photon detector.

For resonant excitation, femtosecond pulses from the parametric laser oscillator were transformed using a 4f pulse shaper [34] to fine-tune the wavelength and pulse duration. The chosen duration of 16 ps ensures optimal laser filtering efficiency and single-photon purity. In the picowatt range, this pulse contains several tens of coherent photons. The spectral width of the laser pulse is  $\sim 77$   $\mu\text{eV}$ . The cavity mode width  $\sim 118$   $\mu\text{eV}$ , determined from the reflectance spectra measured from the top of the micropillar, is slightly wider to allow the laser pulse to propagate without distortion.

The InAs/GaAs QDs suffer from blinking even under resonant excitation [35]. This blinking is particularly pronounced near  $1\pi$ -pulse excitation, where the emission intensity drops below the levels observed at higher  $\pi$ -multiplicity. This leads to a seeming increase in the peak values of the Rabi oscillations, as previously observed in [19, 24]. To reconstruct the true Rabi oscillation profile, we quantified the QD bright state occupancy probability for each power using long-term autocorrelation function measurements [36] and normalized the raw data by this parameter. These corrected graphs are shown in Fig. 1d and Fig. 2c together with theoretical calculations in the main text.

To obtain the dependence of the scattered laser photon intensity on the pulse power shown in Fig. 1d (main text), we measured time-resolved PL decay curves for each power value. Each of these curves was then decomposed into a fast component associated with the laser and slow decaying trion emission (see, e.g., Fig. 1e, main text). The plot of the integrated intensity of the fast components gives the dependence we are looking for.

The energy-detuning experiment was performed using different shifts of the cavity mode energy and the trion energy. The temperature was increased by only about 10 K to  $\sim 20$  K to prevent significant disruption of the photon emission process. During this experiment, the pulse area and duration were kept constant and the laser energy followed the QD energy. To find the dependence of the trion decay on detuning, we increased the temperature to 37 K to achieve complete decoupling between the QD and the cavity and measured the trion lifetime unaffected by the Purcell effect.

## Appendix B: Master equation for trion dynamics with phonons

The full Hamiltonian describing the trion dynamics under light pumping with phonons present consists of three components:  $\hat{H} = \hat{H}_0 + \hat{H}_p + \hat{H}_i$ . Following the established procedure [28], we treat phonon-induced dephasing using second-order perturbation theory. From here on we assume  $\hbar = 1$  in equations. Transforming to the interaction picture with respect to  $\hat{H}_0$  and  $\hat{H}_p$ , and tracing over the phonon bath yields the density matrix equation

$$\begin{aligned} \frac{\partial \hat{\rho}_t}{\partial t} = & -i \left[ \hat{H}_0; \hat{\rho}_t \right] - \\ & - \int_{-\infty}^t d\tau \text{Tr}_p \left( \left[ \hat{H}_i(t_p); \left[ \hat{H}_i(\tau_p, \tau - t_0); \hat{\rho}_t \hat{\rho}_p \right] \right] \right), \\ \hat{H}_i(\tau_p, t_0) = & e^{i(\hat{H}_0 t + \hat{H}_p \tau)} \hat{H}_i e^{-i(\hat{H}_0 t + \hat{H}_p \tau)}. \end{aligned} \quad (\text{B1})$$

When the phonon-induced decay rate remains small compared to the Rabi frequency ( $\gamma \ll \Omega_R$ ), we can replace the photon operators in the decay terms by their average values, effectively using the classical Rabi frequency  $\Omega_R = g\sqrt{N}$ . The density matrix can be represented in the non-trionic/trionic subspace as a  $2 \times 2$  matrix, where each element contains states with different photon numbers. The master Lindblad equation then becomes

$$\frac{\partial \hat{\rho}_t}{\partial t} = -i \left[ \hat{H}_0, \hat{\rho}_t \right] - \hat{\mathcal{L}}(\hat{\rho}_t), \quad (\text{B2})$$

$$\hat{\mathcal{L}}(\hat{\rho}_t) = \gamma [\hat{\sigma}_z, [\hat{\sigma}_z, \hat{\rho}_t]] - \varepsilon [\hat{\sigma}_z, [\hat{\sigma}_y, \hat{\rho}_t]], \quad (\text{B3})$$

$$\gamma = \int_0^\infty \frac{d\tau}{2} \cos(\Omega_R \tau) \int d\omega J_p(\omega) n_\omega \cos(\omega \tau), \quad (\text{B4})$$

$$\varepsilon = \int_0^\infty \frac{d\tau}{2} \sin(\Omega_R \tau) \int d\omega J_p(\omega) n_\omega \cos(\omega \tau), \quad (\text{B5})$$

where,  $J_p(\omega) = \sum_k t_k^2 \delta(\omega - \omega_k)$  represents the trion-phonon coupling strength [28],  $n_\omega$  is the phonon distribution function.

In the absence of dephasing ( $\mathcal{L} = 0$ ), the solution reduces to the coherent case  $\hat{\rho} = \hat{S}_0 \hat{\rho}_0 \hat{S}_0^\dagger$  discussed previously. The primary theoretical challenge arises from mixing states with different photon numbers. For weak dephasing ( $\gamma, \varepsilon \ll \Omega_R$ ) we take this into account by transforming into an interaction picture that yields

$$\frac{\partial \hat{\chi}}{\partial t} = -e^{i\hat{H}_0 t} \mathcal{L} \left[ e^{-i\hat{H}_0 t} \hat{\chi} e^{i\hat{H}_0 t} \right] e^{-i\hat{H}_0 t}. \quad (\text{B6})$$

Averaging over the period of Rabi oscillations  $\theta$  for small damping gives

$$\frac{\partial \hat{\chi}}{\partial t} = i\varepsilon [\hat{\sigma}_x; \hat{\chi}] - \gamma \begin{pmatrix} \chi_{11} - \chi_{22} & 3\chi_{12} + \chi_{21} \\ 3\chi_{21} + \chi_{12} & \chi_{22} - \chi_{11} \end{pmatrix}. \quad (\text{B7})$$

The  $\varepsilon$  term can be eliminated by redefining  $\hat{H}_0 \rightarrow \hat{H}_0 - \varepsilon \hat{\sigma}_x$ , which corresponds to a small correction of the Rabi frequency. For the initial condition where only the

$\chi_z$  component is non-zero, corresponding to the coherent pump pulse (2), we obtain the solution

$$\hat{\rho}_t = \frac{1}{2} \hat{S}_1 \left( \hat{I} + \hat{\sigma}_z e^{-2\gamma t} \right) |\Psi_{\text{in}}\rangle \langle \Psi_{\text{in}}| \hat{S}_1^\dagger, \quad (\text{B8})$$

$$\hat{S}_1 = \exp \left[ -it \begin{pmatrix} 0 & g\hat{b}_- - \varepsilon \\ g\hat{b}_-^\dagger - \varepsilon & 0 \end{pmatrix} \right].$$

Following the pulse interaction ( $t \rightarrow \tau$ ), the trion undergoes radiative decay, requiring the replacement  $\hat{a}_+|0\rangle \rightarrow \hat{b}_-^\dagger|0\rangle$  in the density matrix.

### Appendix C: Dependence of interaction strength and time on detuning

To get how the detuning affects the interaction time  $\tau$  and its strength  $\delta$ , we need to determine the interaction constant  $g$  in Eq. (1) (main text) from the microscopic values. The interaction of a trion with a photon mode  $\omega$  is:

$$g_\omega = g_* \left( \frac{i\sqrt{\Gamma/\pi}}{\nu_0 - \omega + i\Gamma} + \sqrt{\nu_0} \right), \quad (\text{C1})$$

where  $g_*$  - bare interaction constant (measured in energy units),  $\nu_0$  - photon density of states out of cavity resonance. The trion excitation time is:  $1/\tau_t \sim |g_{E_t}|^2$ . When pumping the system, the laser envelope must be taken into account, and  $g$  in equation (1) is:  $g(t) = \int d\omega \alpha_\omega g_\omega e^{i(\omega - \omega_L)t}$ , where  $\alpha_\omega$  is the pump laser amplitude, centered on  $\omega_L$  and having a width of  $1/\tau_p$ . The evolution operator contains an interaction constant integrated over the interaction time:

$$\delta \sim \int dt g(t) \sim g_* \left( \frac{i\sqrt{\Gamma\tau_p}}{\Delta + i\Gamma} + \sqrt{\nu_0\tau_p} \right). \quad (\text{C2})$$

The Rabi frequency, which is determined by the rate of the dephasing caused by phonons, is

$$\frac{\Omega_R}{\sqrt{N}} = g(t=0) \sim g_* \left( \frac{i\sqrt{\Gamma/\tau_p}}{\Delta + i(\Gamma + 1/\tau_p)} + \sqrt{\nu_0/\tau_p} \right).$$

A simulation of the experimental Rabi oscillations using this approach is shown in Fig. 2c (main text). The interaction time  $\tau(\Delta)$ , relevant for phonon dephasing under detuning, is given by

$$\tau(\Delta) = \left| \frac{\int dt g(t)}{g(t=0)} \right|. \quad (\text{C3})$$

For example, without detuning and neglecting  $\nu_0$ :  $\tau(\Delta = 0, \nu_0 = 0) = \tau_p + 1/\Gamma = \max(\tau_p, \Gamma^{-1})$ , as defined earlier. Substituting eqs. (C2) and (C3) into eq. (6) gives the dependence of the second-order correlation function at  $\theta = 2\pi$  on the detuning.

The procedure for fitting the experimental data presented in Fig. 2 is as follows:

(i) First, we derive from the Rabi oscillations (Fig. 2c) the frequency correction  $\tilde{\theta}$  extended by a second-order term  $\tilde{\theta} \approx \theta + a\theta^2$  and the phonon-induced decay  $\gamma\tau \approx b\theta^2$  (for the weak coupling regime).

(ii) Then, we simulated the function  $g^{(2)}(0)$  as a function of the pulse area to determine the coupling strength  $\delta$  and the incoherent admixture  $\lambda$ , which is assumed to consist mainly of single (rather than multiple) photons. As a result, the noise parameters are reduced to a single parameter  $\lambda$  with  $\gamma_1 = 2\lambda/(1 - \lambda)$  and  $\gamma_2 = 0$ .

(iii) Next, we fit the dependence of the trion time on the detuning (Fig. 2a) and obtain the parameter  $\Gamma\nu_0$ .

Finally, we construct the dependence of  $g^{(2)}(0)$  at  $\theta = 2\pi$  on the detuning (Fig. 2b), using the found parameters and the relation  $\Gamma\tau_p$  between the resonator width and the pulse duration.

- 
- [1] P. Senellart, G. Solomon, and A. White, High-performance semiconductor quantum-dot single-photon sources, *Nature Nanotechnology* **12**, 1026 (2017).
- [2] N. Tamm, A. Javadi, N. Antoniadis, D. Najer, M. Lobl, A. Korsch, R. Schott, S. Valentin, A. Wieck, A. Ludwig, and R. Warburton, A bright and fast source of coherent single photons, *Nature Nanotechnology* **16**, 399–403 (2021).
- [3] M. Rakhlin, A. Galimov, I. Dyakonov, N. Skryabin, G. Klimko, M. Kulagina, Y. Zadiranov, S. Sorokin, I. Sedova, Y. Guseva, D. Berezina, Y. Serov, N. Maleev, A. Kuzmenkov, S. Troshkov, K. Taratorin, A. Skalkin, S. Straupe, S. Kulik, T. Shubina, and A. Toropov, Demultiplexed single-photon source with a quantum dot coupled to microresonator, *Journal of Luminescence* **253**, 119496 (2023).
- [4] K. Tiurev, M. H. Appel, P. L. Mirambell, M. B. Lauritzen, A. Tiranov, P. Lodahl, and A. S. Sørensen, High-fidelity multiphoton-entangled cluster state with solid-state quantum emitters in photonic nanostructures, *Physical Review A* **105**, L030601 (2022).
- [5] H. Huet, P. R. Ramesh, S. C. Wein, N. Coste, P. Hilaire, N. Somaschi, M. Morassi, A. Lemaître, I. Sagnes, M. F. Doty, O. Krebs, L. Lanco, D. A. Fioretto, and P. Senellart, Deterministic and reconfigurable graph state generation with a single solid-state quantum emitter, *Nature Communications* **16**, 4337 (2025).
- [6] D. M. Greenberger, M. A. Horne, A. Shimony, and A. Zeilinger, Bell's theorem without inequalities, *American Journal of Physics* **58**, 1131–1143 (1990).
- [7] E. Knill, R. Laflamme, and G. J. Milburn, A scheme for efficient quantum computation with linear optics, *Nature* **409**, 46–52 (2001).
- [8] T. C. Ralph, A. Gilchrist, G. J. Milburn, W. J. Munro,

- and S. Glancy, Quantum computation with optical coherent states, *Physical Review A* **68**, 042319 (2003).
- [9] A. Ourjoumtsev, H. Jeong, R. Tualle-Brouri, and P. Grangier, Generation of optical ‘Schrödinger cats’ from photon number states, *Nature* **448**, 784–786 (2007).
- [10] I. Afek, O. Ambar, and Y. Silberberg, High-NOON states by mixing quantum and classical light, *Science* **328**, 879–881 (2010).
- [11] W.-Y. Hwang, Quantum key distribution with high loss: Toward global secure communication, *Physical Review Letters* **91**, 057901 (2003).
- [12] C. Matthiesen, A. N. Vamivakas, and M. Atatüre, Sub-natural linewidth single photons from a quantum dot, *Physical Review Letters* **108**, 093602 (2012).
- [13] A. J. Bennett, J. P. Lee, D. J. P. Ellis, I. Farrer, D. A. Ritchie, and A. J. Shields, A semiconductor photon-sorter, *Nature Nanotechnology* **11**, 857–860 (2016).
- [14] X.-J. Wang, G. Huang, M.-Y. Li, Y.-Z. Wang, L. Liu, B. Wu, H. Liu, H. Ni, Z. Niu, W. Ji, R. Jiao, H.-L. Yin, and Z. Yuan, Coherence in resonance fluorescence (2025), arXiv:2312.13743 [quant-ph].
- [15] A. Müller, E. B. Flagg, P. Bianucci, X. Y. Wang, D. G. Deppe, W. Ma, J. Zhang, G. J. Salamo, M. Xiao, and C. K. Shih, Resonance fluorescence from a coherently driven semiconductor quantum dot in a cavity, *Physical Review Letters* **99**, 187402 (2007).
- [16] A. V. Kuhlmann, J. H. Prechtel, J. Houel, A. Ludwig, D. Reuter, A. D. Wieck, and R. J. Warburton, Transform-limited single photons from a single quantum dot, *Nature Communications* **6**, 8204 (2015).
- [17] A. I. Galimov, M. V. Rakhlin, G. V. Klimko, Y. M. Zadiranov, Y. A. Guseva, S. I. Troshkov, T. V. Shubina, and A. A. Toropov, Source of indistinguishable single photons based on epitaxial InAs/GaAs quantum dots for integration in quantum computing schemes, *JETP Letters* **113**, 252–258 (2021).
- [18] C. S. Muñoz, E. del Valle, A. G. Tudela, K. Müller, S. Lichtmannecker, M. Kaniber, C. Tejedor, J. J. Finley, and F. P. Laussy, Emitters of N-photon bundles, *Nature Photonics* **8**, 550–555 (2014).
- [19] K. Fischer, L. Hanschke, J. Wierzbowski, T. Simmet, C. Dory, J. Finley, J. Vučković, and K. Müller, Signatures of two-photon pulses from a quantum two-level system, *Nature Physics* **13**, 649–654 (2017).
- [20] E. del Valle, A. Gonzalez-Tudela, F. P. Laussy, C. Tejedor, and M. J. Hartmann, Theory of frequency-filtered and time-resolved N-photon correlations, *Physical Review Letters* **109**, 183601 (2012).
- [21] E. Zubizarreta Casalengua, J. C. López Carreño, F. P. Laussy, and E. del Valle, Tuning photon statistics with coherent fields, *Physical Review A* **101**, 063824 (2020).
- [22] L. Hanschke, L. Schweickert, J. C. L. Carreño, E. Schöll, K. D. Zeuner, T. Lettner, E. Z. Casalengua, M. Reindl, S. F. C. da Silva, R. Trotta, J. J. Finley, A. Rastelli, E. del Valle, F. P. Laussy, V. Zwiller, K. Müller, and K. D. Jöns, Origin of antibunching in resonance fluorescence, *Physical Review Letters* **125**, 170402 (2020).
- [23] S. K. Kim, E. Z. Casalengua, K. Boos, F. Sbresny, C. Calcagno, H. Riedl, J. J. Finley, C. Antón-Solanas, F. P. Laussy, K. Müller, L. Hanschke, and E. del Valle, Unlocking multiphoton emission from a single-photon source through mean-field engineering (2024), arXiv:2411.10441 [quant-ph].
- [24] J. C. Loredó, C. Antón, B. Reznichenko, P. Hilaire, A. Harouri, C. Millet, H. H. Ollivier, N. Somaschi, L. De Santis, A. Lemaitre, I. Sagnes, L. Lanco, A. Auffeves, O. Krebs, and P. Senellart, Generation of non-classical light in a photon-number superposition, *Nature Photonics* **13**, 803–808 (2019).
- [25] K. A. Fischer, L. Hanschke, M. Kremser, J. J. Finley, K. Müller, and J. Vučković, Pulsed Rabi oscillations in quantum two-level systems: beyond the area theorem, *Quantum Science and Technology* **3**, 014006 (2017).
- [26] Y. Serov, A. Galimov, D. S. Smirnov, M. Rakhlin, N. Leppänen, G. Klimko, S. Sorokin, I. Sedova, D. Berezina, Y. Saliı̄, M. Kulagina, Y. Zadiranov, S. Troshkov, T. V. Shubina, and A. A. Toropov, Hidden anisotropy controls spin-photon entanglement in a charged quantum dot, *Physical Review Applied* **23**, 044019 (2025).
- [27] A. J. Ramsay, A. V. Gopal, E. M. Gauger, A. Nazir, B. W. Lovett, A. M. Fox, and M. S. Skolnick, Damping of exciton Rabi rotations by acoustic phonons in optically excited InGaAs/GaAs quantum dots, *Phys. Rev. Lett.* **104**, 017402 (2010).
- [28] A. Nazir and D. P. S. McCutcheon, Modelling exciton–phonon interactions in optically driven quantum dots, *Journal of Physics: Condensed Matter* **28**, 103002 (2016).
- [29] A. J. Ramsay, T. M. Godden, S. J. Boyle, E. M. Gauger, A. Nazir, B. W. Lovett, A. M. Fox, and M. S. Skolnick, Phonon-induced Rabi-frequency renormalization of optically driven single InGaAs/GaAs quantum dots, *Phys. Rev. Lett.* **105**, 177402 (2010).
- [30] C. Arnold, J. Demory, V. Loo, A. Lemaitre, I. Sagnes, M. Glazov, O. Krebs, P. Voisin, P. Senellart, and L. Lanco, Macroscopic rotation of photon polarization induced by a single spin, *Nature Communications* **6**, 6236 (2015).
- [31] P. Androvitsaneas, A. B. Young, C. Schneider, S. Maier, M. Kamp, S. Höfling, S. Knauer, E. Harbord, C. Y. Hu, J. G. Rarity, and R. Oulton, Charged quantum dot micropillar system for deterministic light-matter interactions, *Phys. Rev. B* **93**, 241409 (2016).
- [32] E. Mehdi, M. Gundín, C. Millet, N. Somaschi, A. Lemaitre, I. Sagnes, L. Le Gratiet, D. A. Fioretto, N. Belabas, O. Krebs, P. Senellart, and L. Lanco, Giant optical polarisation rotations induced by a single quantum dot spin, *Nature Communications* **15**, 598 (2024).
- [33] A. I. Galimov, Y. M. Serov, M. V. Rakhlin, G. V. Klimko, S. V. Sorokin, I. V. Sedova, M. M. Kulagina, Y. M. Zadiranov, Y. A. Saliı̄, D. S. Berezina, S. I. Troshkov, T. V. Shubina, and A. A. Toropov, Charge states of single quantum dots in a microcavity p–n–p heterostructure with the built-in Coulomb blockade, *JETP Letters* **121**, 365–371 (2025).
- [34] A. Monmayrant, S. Weber, and B. Chatel, A newcomer’s guide to ultrashort pulse shaping and characterization, *Journal of Physics B-atomic Molecular and Optical Physics* **43**, 103001 (2010).
- [35] H. S. Nguyen, G. Sallen, M. Abbarchi, R. Ferreira, C. Voisin, P. Roussignol, G. Cassaboıs, and C. Diederichs, Photoneutralization and slow capture of carriers in quantum dots probed by resonant excitation spectroscopy, *Physical Review B* **87**, 115305 (2013).
- [36] P. Hilaire, C. Millet, J. C. Loredó, C. Antón, A. Harouri, A. Lemaitre, I. Sagnes, N. Somaschi, O. Krebs, P. Senellart, and L. Lanco, Deterministic assembly of a charged-quantum-dot–micropillar cavity device, *Phys. Rev. B*

102, 195402 (2020).